SHORT COMMUNICATION
62nd STAPP CAR CRASH CONFERENCE
SC18-07

Human Surrogate Finite Element Models under Multi-Directional Loading: Applications of Aerospace Data for the Future of Automotive Environments

James P. Gaewsky, Derek A. Jones, Xin Ye, Bharath Koya, Kyle P. McNamara, Mona Z. Saffarzadeh, F. Scott Gayzik, Ashley A. Weaver, Joel D. Stitzel
Virginia Tech – Wake Forest Center for Injury Biomechanics

ABSTRACT – Injury biomechanics for the automotive environment of the future may be influenced by biomechanical analyses from other fields, including the aerospace environment. This short communication studied the influence of loading direction on the head, neck and lumbar responses of three human surrogate finite element models (Hybrid III, THOR and the simplified GHBMC 50th percentile male) subjected to low-to-moderate acceleration pulses in approximately 25+ frontal (-X), rear (+X), vertical (+Z and -Z), and lateral (+Y) pulses from a design of experiments to simulate water landings of spacecraft. Pulse magnitudes ranged from 5-25 G. BrIC, neck compression, and lumbar compression forces were cross compared between the three models for each of the five loading directions. The comparison between HIII and GHBMC lumbar forces indicated that GHBMC overestimated lumbar forces in simulations in the primarily -X loading direction compared to HIII, while in the other loading directions it typically underestimated. The results of this study help to elucidate the sensitivity and extensibility of these human surrogate finite element models across injury metrics and loading directions.

INTRODUCTION

Passenger vehicles on the roads today are designed with occupants positioned in upright, forward-facing seats. However, advances in automated driving have led to recent concept designs and discussions related to off-nominal seating configurations in passenger vehicles of the future (Cuddihy and Rao 2016). In the event of motor vehicle collisions involving super-reclined occupant seating configurations, it is expected that the relative load in the occupant's vertical direction would exceed the load in the occupant's horizontal plane. In combination with novel occupant seating configurations, automated driving will reduce the mean impact speeds and pulse severities in the event of collision. It will be important to understand the biomechanical responses and shortcomings of existing experimental and finite element tools in the loading conditions of future generations of passenger vehicles. However, the loading conditions of future generations of vehicles may have more similarities to other transportation environments than modern motor vehicles. This work leverages biomechanical data from finite element models subjected to an array of aerospace accelerative loading to understand the response differences between human surrogate models in off-nominal passenger vehicle seating configurations.

METHODS

Occupant Models

In this study, three 50th percentile male occupant finite element models (Humanetics Hybrid III, NASA THOR, and GHBMC M50-OS) were subjected to complex acceleration pulses derived from aerospace loading conditions with combined loading direction components. The kinematics of these models, positioned and belted in 90°-90°-90° hip-knee-ankle configurations, were first validated against uni-directional frontal (-X), rear (+X), vertical (+Z), and lateral (±Y) experimental tests available through the Air Force Research Lab's Biodynamics Databank (McNamara, Jones et al. 2017; Ye, Jones et al. 2017). Validation of the GHBMC model was performed in 13 unique loading conditions, while the HIII model was validated in 25 loading conditions and the THOR model was validated in 11 loading conditions.

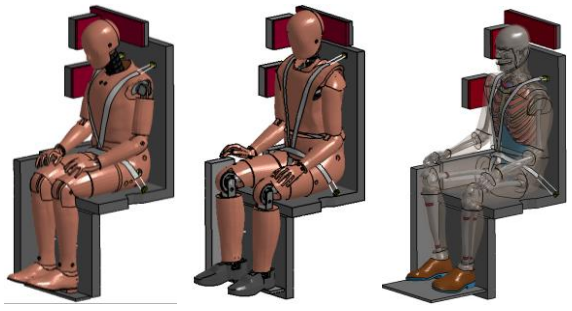

Figure 1: Belted and settled (a) Hybrid III, (b) THOR, and (c) GHBMC M50-OS.

Each validated model was positioned into a seat with a flat seat pan and seat back without padding, and a head rest with minimal padding (Figure 1). The seat back and seat legs were oriented 90° to the seat pan, and a foot rest was included. A selection of side guards were implemented on one side of the seat model.

Address correspondence to James P. Gaewsky,
575 N. Patterson Ave Suite 120, Winston-Salem, NC 27101.
Electronic mail: jgaewsky@wakehealth.edu

Design of Experiments

For each occupant model a Latin hypercube study (LHS) design of experiments (DOE) was performed to analyze the sensitivity of the model inputs on calculated injury metrics and risks. A total of 455 experimental samples using 13 independent variables were generated for each LHS. The 13 independent variables were categorized into "loading condition variables", which were defined during the loading phase of the simulation, and "environmental simulation variables", which were defined during the settling phase and summarized in Table .

Across the three occupant models, the same set of 455 pulses was applied. Each pulse was described by independent X-, Y-, and Z-components that were each characterized by shape and magnitude parameters. The pulse shape rise times ranged from 32.5 ms to 120 ms. The relative size parameters describe the loading direction. The resultant of the scaled component pulses was subsequently scaled to have peak acceleration equal to the remaining loading condition parameter from the LHS (5 to 25 G). The resulting applied acceleration pulse conditions are summarized in Figure 2.

Two environmental parameters defined the orientation of the occupant's environment during pulse application. The rotation of the model about the local Y-axis (at the hip/H-point) ranged from -45° to +45° and about the local Z-axis (spinal direction), from 0 to 20°. Two additional parameters were used to define the offset of the occupant model from the seat pan (Z-offset) and seat back (X-offset) at the initiation of the settling phase. Another parameter defined the force to which the seatbelts are tightened, ranging from 5 to 35 lbf (22.2 to 155 N).

Loading Condition Comparison

Groupings of simulations from the LHS of each occupant model were selected to create a subsampling for five different approximate principal loading directions (SAE J211: frontal, (-X, n=28), rear (+X , n=27), downward (-Z , n=26), spinal, (+Z, n=26) and lateral (+Y, n=46)) by selecting simulations with peak accelerations within a 30° cone of the loading direction (Figure 2). Each LHS used the same set of pulses, in order to compare injury metric values as matched pairs between occupant models.

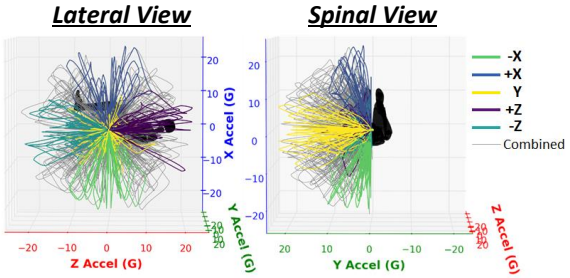

Figure 2: Summary of 455 applied pulses for each of the three occupant models and the selected simulations for local principal direction of force.

Table 1. LHS Variables Ranges.

	LHS Input Variables	Minimum	Maximum	Derived Analysis Variables
Loading Condition Variables	**X** (longitudinal) Pulse Shape	0	1	**X** Pulse Rise Time (32.5→120 ms)
	Y (lateral) Pulse Shape	0	1	**Y** Pulse Rise Time (32.5→120 ms)
	Z (vertical) Pulse Shape	0	1	**Z** Pulse Rise Time (32.5→120 ms)
	X (longitudinal) Direction Component	-1 (frontal impact)	1 (rear impact)	Peak X-, Y-, Z-Component Acceleration (G)
	Y (lateral) Direction Component	0	1	
	Z (vertical) Direction Component	-1 (impact from above)	1 (impact from below)	
	Resultant Pulse Magnitude	5 G	25 G	
Simulation Environment Variables	**Y**-axis Model Rotation	-45°	45°	
	Z-axis Model Rotation	0°	20°	
	X-offset of Model from Seat	0 mm	20 mm	Settled Hip/H-Point **X,Z**-location and angle
	Z-offset of Model from Seat	0 mm	20 mm	
	Seatbelt Tension Force	5 N (22.2 lbf)	35 N (155 lbf)	

RESULTS

Three injury metrics, BrIC, neck compression force and lumbar compression force were compared between the three human body surrogate models for each of the five loading directions. Lumbar data is plotted in Figure 3 with the top left subplot comparing GHBMC L1-L2 joint force to THOR, the bottom left comparing Hybrid III (HIII) to THOR and the bottom right comparing GHBMC to HIII. Summary slopes of the fitted trend lines are summarized in the top right table. Slopes closest to 1 corresponded to agreement in measured injury metrics between models.

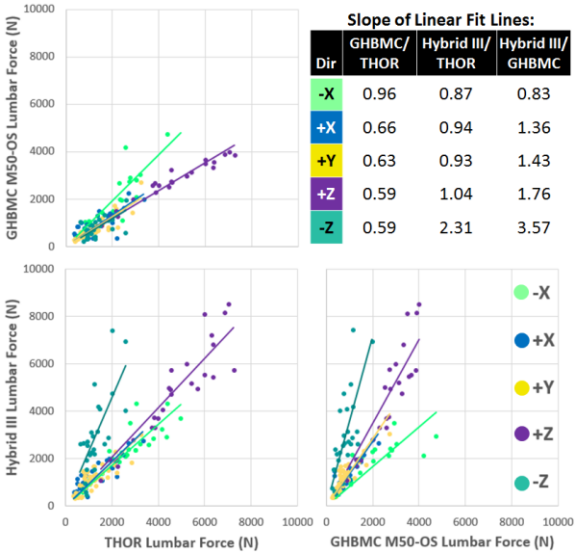

Figure 3: (Top Left) GHBMC vs. THOR lumbar force. (Bottom Left) HIII vs. THOR lumbar force. (Bottom Right) HIII vs. GHBMC lumbar force.

Additionally, the slopes of the trend lines between occupant models are summarized in Table 2.

Table 2. Slope of linear fit lines between occupant models.

	BrIC			Neck Compression		
	GHBMC/ THOR	HIII/ THOR	HIII/ GHBMC	GHBMC/ THOR	HIII/ THOR	HIII/ GHBMC
-X	0.86	0.69	0.81	0.86	0.33	0.23
+X	0.82	0.51	0.57	0.79	0.70	6.71
+Y	0.45	0.51	0.82	0.49	0.86	1.64
+Z	1.05	0.95	0.83	0.45	0.89	2.07
-Z	0.52	0.52	1.01	0.89	0.46	0.21

DISCUSSION

As seen in Figure 3, loading direction has a varying influence on the magnitude of resulting lumbar force measurements depending on the occupant model. If each model predicted the same lumbar force in paired simulations, then the trend lines for each loading direction would all have slopes of 1. The comparison between HIII and GHBMC lumbar forces indicated that GHBMC overestimated lumbar forces in simulations in the primarily -X loading direction compared to HIII, while in the other loading directions it typically underestimated. As seen in Table 2, THOR typically overestimated BrIC compared to the other two models in the +Y loading direction. Also notably, GHBMC underestimated neck compression force compared to the two ATD models in the +X, +Y, and +Z direction simulations.

A limitation of this dataset for traffic safety implications was that it used a rigid, 90° seat and a 5-point seatbelt harness which would restrict excursion of the occupant significantly more than modern passenger vehicle safety measures. Additionally, differences in model geometry make it impossible to create identically positioned models.

CONCLUSION

The results of this study help to elucidate the types of complex loading conditions that human body models and computational models of ATDs perform most similarly. It also helps to understand the sensitivity and extensibility of these human surrogate finite element models across injury metrics and loading directions. This information will lead to further improvement of the models and allow for them to be used appropriately in future simulations of aerospace and automotive environments.

ACKNOWLEDGMENTS

This study was supported by NASA Human Health and Performance Contract (HHPC) through KBRwyle. Views expressed are those of the authors and do not represent the views of NASA or KBRwyle. Simulations were performed on the Wake Forest DEAC cluster, a centrally managed resource with support provided in part by the university.

REFERENCES

Cuddihy, M. A. and M. K. Rao (2016). Autonomous vehicle with reconfigurable seats, Google Patents.

McNamara, K., D. Jones, et al. (2017). Validating FE Hybrid III And THOR For Future Spaceflight Configuration Testing. Biomedical Engineering Society Annual Meeting, Phoenix, AZ.

Ye, X., D. Jones, et al. (2017). Validation Of A Finite Element Human Body Model For Spaceflight Testing Configurations. Biomedical Engineering Society Annual Meeting, Phoenix, AZ.